

HNPS Advances in Nuclear Physics

Vol 30 (2024)

HNPS2023

HNPS: Advances in Nuclear Physics

31st Hellenic Conference

Editors: M. Diakaki, M. Kokkoris, V. Michalopoulou, R. Vlastou

HNPS: Advances in Nuclear Physics

Editors
M. Diakaki
M. Kokkoris
V. Michalopoulou
R. Vlastou

Proceedings of the
31st Hellenic
Conference
on Nuclear Physics
National Technical
University of Athens
Sep 29th - Sep 30th 2023

Hellenic Nuclear
Physics Society

**Radio-dating method of ^{210}Pb in a marine
sediment core from the deep basin Northern of
Skyros Isl., Aegean Sea**

*Spyridoula - Konstantina Roumelioti, Dionysios Patiris,
Christos Tsabarlis, Stylianos Alexakis*

doi: [10.12681/hnpsanp.6286](https://doi.org/10.12681/hnpsanp.6286)

Copyright © 2024, Spyridoula - Konstantina Roumelioti, Dionysios Patiris, Christos Tsabarlis, Stylianos Alexakis



This work is licensed under a [Creative Commons Attribution-NonCommercial-NoDerivatives 4.0](https://creativecommons.org/licenses/by-nc-nd/4.0/).

To cite this article:

Roumelioti, S. - K., Patiris, D., Tsabarlis, C., & Alexakis, S. (2024). Radio-dating method of ^{210}Pb in a marine sediment core from the deep basin Northern of Skyros Isl., Aegean Sea. *HNPS Advances in Nuclear Physics*, 30, 241-245.
<https://doi.org/10.12681/hnpsanp.6286>

Radio-dating method of ^{210}Pb in a marine sediment core from the deep basin Northern of Skyros Island, Aegean Sea

S.K. Roumelioti^{1,2}, D.L. Patiris^{1,*}, C. Tsabarlis¹, S. Alexakis¹

¹ Institute of Oceanography, Hellenic Centre for Marine Research, 19013, Anavyssos, Greece

² Department of Physics, National Technical University of Athens, 15780, Athens, Greece

Abstract In this work, the level of natural and artificial radioactivity in a marine sediment core obtained from the Northern basin of Skyros (Sporades region - Aegean Sea, Greece) was measured by a high-purity germanium detector. More specifically, the activity concentration was determined for the radionuclides ^{226}Ra , ^{214}Pb , ^{214}Bi and ^{210}Pb , ^{208}Tl , and ^{228}Ac , the natural potassium radioisotope ^{40}K , and the anthropogenic cesium radionuclide ^{137}Cs . The vertical distribution was obtained for each of them in the core and subsequently, based on the radio-dating method of ^{210}Pb , the time reconstruction of their activity was realized. The sediment accumulation rate was calculated at $(0.17 \pm 0.02) \text{ cm y}^{-1}$ which in the specific core is equivalent to sediment deposition of 1cm per (6 ± 1) years. The vertical distribution of ^{137}Cs was also used to validate the accumulation rate. According to the time reconstruction, a significant increase of both ^{226}Ra and ^{208}Tl was revealed in the period 1950-1960. The results highlight that the radio dating method of ^{210}Pb , even though it is widely used in coastal marine areas, can be successfully applied in deep-sea regions where the accumulation of sediment is high enough (mm per year) due to sediment gravity flow.

Keywords environmental radioactivity, accumulation rate, gamma-ray spectrometry

INTRODUCTION

The aim of this work was the study of the deep sea and specifically the comprehension of phenomena that take place in the deep basins of the North Aegean and the evaluation of the possibility of utilizing radio-tracing methods that are already used in the coastal environments. The study of the vertical distribution of the activity concentration of natural and anthropogenic radionuclides was performed deducing the accumulation rate of the sediment in the study area.

For the measurements, a sediment core was sampled in September 2020 from the Northern basin of Skyros. The core was cut into individual slices and the levels of natural and artificial radioactivity of each unit were determined with gamma-spectroscopy. The measurements were performed using a calibrated high-purity germanium (HPGe) detector of the HCMR laboratory providing the vertical distribution of the activity concentration of the radionuclides. By using a dating model based on lead ^{210}Pb , the deposition rate of the sediment in this area was estimated and a time calibration of the vertical distribution of radionuclides in the sediment core was performed.

EXPERIMENTAL DETAILS

The sediment core was taken from about 1020 m ($39^{\circ} 1'12.00''\text{N}$ $24^{\circ}41'24.00''\text{E}$) (Fig. 1). It was separated into samples of 1 cm thickness and after 20 cm to 2 cm thickness. Initially, the samples were placed in an oven, until all the water evaporates and only the dry mass of the sample remains. The mass of the dried samples was then measured and pulverized using an agate mortar. They were placed in cylindrical containers and the activity concentration (C) of each one was calculated after the measurement of the sediment mass (m) and the activity (A). The latter was defined by the following equation:

* Corresponding author: dpatiris@hcmr.gr

$$A = \frac{\text{counts}}{I_\gamma \cdot \text{FEPE} \cdot \text{time} \cdot m} \quad (1)$$

where, *counts*: the experimental counts, calculated from the spectra, with the SPECTRW software, *FEPE*: the full-energy peak efficiency, calculated from the fitted function, I_γ : the emission probability of the gamma-ray, *time*: the time measurement of the sample (24 hours), *m*: the net mass of the sample (kg).

For the calculation of full-energy peak efficiency (FEPE), two required corrections were applied to the experimental counts of the ^{152}Eu calibration source. The corrections were made utilizing the EFFTRAN code [14] considering the calculation of true coincidence summing correction factors (TCS) for every gamma-ray energy, as well as due to the density difference between the calibration source and the mean density of the samples (due to different self-absorption effects).

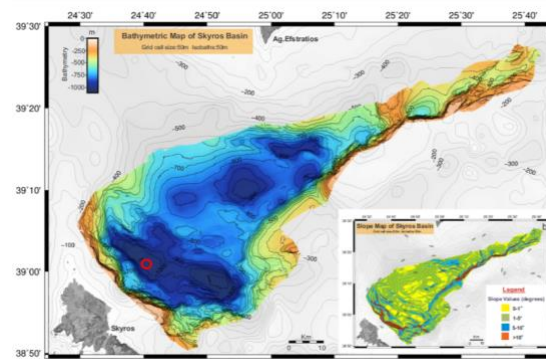


Figure 1. Sediment sampling position from the Northern basin of Skyros

The accumulation rate, which is a result of atmospheric fallout and gravity flows, was estimated in three ways. By ^{210}Pb dating, using two assumptions for the excess activity concentration, and by ^{137}Cs dating. In the first two cases, the accumulation rate was estimated using the distribution of the excess activity concentration of $^{210}\text{Pb}_{\text{ex}}$ by the Constant Flux: Constant Sedimentation (CF: CS) model [12], which assumes that the $^{210}\text{Pb}_{\text{ex}}$ flux to the sediment surface and the sedimentation rate is constant. The activity concentration, *C*, is assumed to depend on the cumulative sediment mass *m*:

$$C(m) = C_0 e^{-\frac{\lambda m}{v}} \Rightarrow \ln C(m) = \ln C_0 - \frac{\lambda}{v} m \quad (2)$$

where, C_0 : the activity concentration of $^{210}\text{Pb}_{\text{ex}}$ for $t=0$, $z=0$, *m*: the mass of the sample, λ : decay constant, *v*: accumulation rate.

The excess activity concentration (*C*) of $^{210}\text{Pb}_{\text{ex}}$ was measured with the following two ways:

1. $^{210}\text{Pb}_{\text{ex},i} = ^{210}\text{Pb}_i - ^{226}\text{Ra}_i$, *i*: the sample depth
2. $^{210}\text{Pb}_{\text{ex},i} = ^{210}\text{Pb}_i - ^{226}\text{Ra}_{\text{av}}$, $^{226}\text{Ra}_{\text{av}}$: average concentration of ^{226}Ra from the depth where it is stable

In the case of ^{137}Cs dating, the method relies on the two characteristic peaks of maximum concentration in the sediment core. The first peak represents 1963, which corresponds to the maximum concentrations in the air because of the nuclear cloud, and the second peak 1986, corresponds to the Chernobyl accident. The occurrence of ^{137}Cs peaks in each core allows the estimation of the average rate of sediment accumulation at the bottom, assuming a linear dependence between peaks along the depth. The mean sedimentation rates (*v_i*) after 1963 and after 1986 are calculated, respectively:

$$v_i = \frac{z_i}{t_0 - t_i} \quad (3)$$

where, *t₀*: the date of the core extraction, *t_i*, *z_i*: depths and dates of high activity concentrations of ^{137}Cs .

RESULTS AND DISCUSSION

The activity concentration of ^{208}Tl ranges from $(29 \pm 5) \text{ Bq kg}^{-1}$ to $(76 \pm 5) \text{ Bq kg}^{-1}$, of ^{228}Ac from $<\text{MDA}$ to $(86 \pm 11) \text{ Bq kg}^{-1}$, and ^{40}K from $(262 \pm 24) \text{ Bq kg}^{-1}$ to $(714 \pm 182) \text{ Bq kg}^{-1}$. We observe that ^{208}Tl and ^{228}Ac behave in the same way, their concentration is almost constant in the first 10 cm, at 10-12 cm there is a slight increase, and below 12 cm of depth, the concentration decreases to the initial range of values and remains almost constant. The activity concentration of ^{40}K exhibits the maximum activity concentration at 1 cm and below that, it decreases and exhibits an almost constant value below 2 cm (see Figure 2). The activity concentration of ^{214}Bi ranges from $<\text{MDA}$ to $(105 \pm 8) \text{ Bq kg}^{-1}$, ^{214}Pb from $<\text{MDA}$ to $(87 \pm 7) \text{ Bq kg}^{-1}$, and ^{226}Ra from $<\text{MDA}$ to $(97 \pm 11) \text{ Bq kg}^{-1}$. The aforementioned radionuclides have the same distribution since ^{214}Pb and ^{214}Bi are daughters of ^{226}Ra . In particular, the value is stable except for 10-12 cm where an increase is observed, which concerns an event that disrupted the constant flux (Figures 2 and 4). The activity values of ^{137}Cs range from $<\text{MDA}$ to $(7 \pm 3) \text{ Bq kg}^{-1}$, $^{210}\text{Pb}_{\text{ex}}$ from $<\text{MDA}$ to $(351 \pm 197) \text{ Bq kg}^{-1}$, and ^{210}Pb from $<\text{MDA}$ to $(368 \pm 196) \text{ Bq kg}^{-1}$. The activity concentration of ^{137}Cs exhibits two non-intense energy peaks and appears to be close to zero at 20 cm and below. The activity concentration of the total and excess ^{210}Pb have constant concentrations in the first 20 cm and below that it appears to be close to zero (Figure 3).

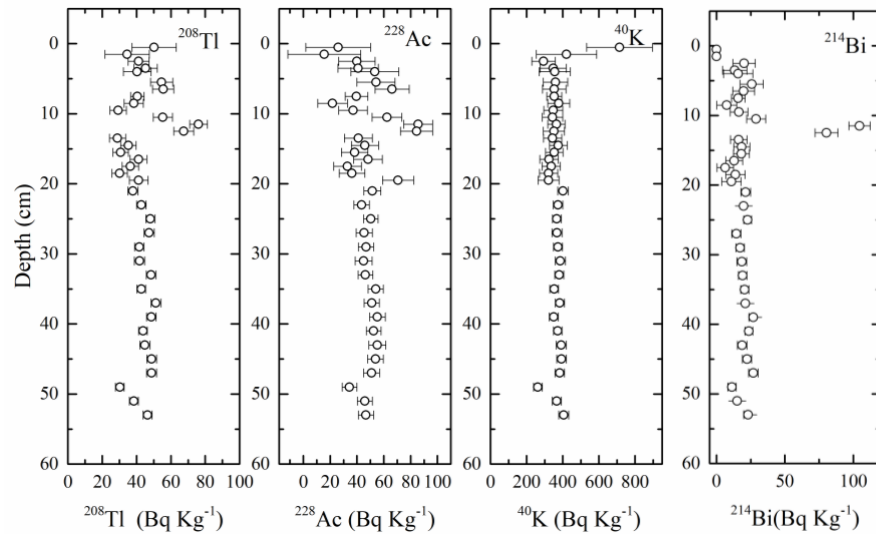


Figure 2. The activity concentration distribution of ^{208}Tl , ^{228}Ac , ^{40}K , ^{214}Bi as a function of core depth

By the ^{210}Pb dating method, the accumulation rate was measured to be $v = (0.17 \pm 0.02) \text{ cm y}^{-1}$ and $v = (0.16 \pm 0.02) \text{ cm y}^{-1}$ for the two assumptions, respectively, while by the ^{137}Cs dating method was found to be $v = (0.12 \pm 0.05) \text{ cm y}^{-1}$. All the accumulation rate values are in very good agreement within errors. Moreover, the activity concentration distribution of ^{226}Ra , calculated based on ^{210}Pb , is presented in Fig. 4 as a function of depth and time.

The estimation of the two accumulation rates differs due to the very low activity concentration of ^{137}Cs (high uncertainty), to the instability of the accumulation rate throughout the decades (especially 1950-1960), to severe geophysical events increasing the gravity flow and the mobility of ^{137}Cs vertically in the sediment core.

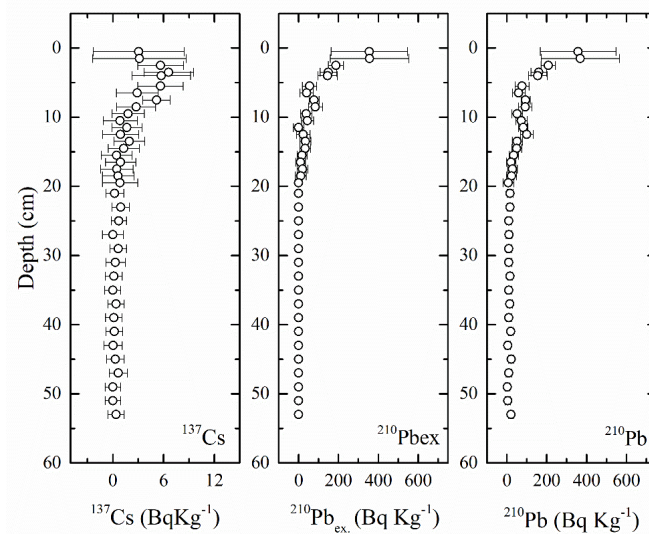


Figure 3. The activity concentration distribution of ^{137}Cs , $^{210}\text{Pb}_{\text{ex}}$, ^{210}Pb as a function of core depth

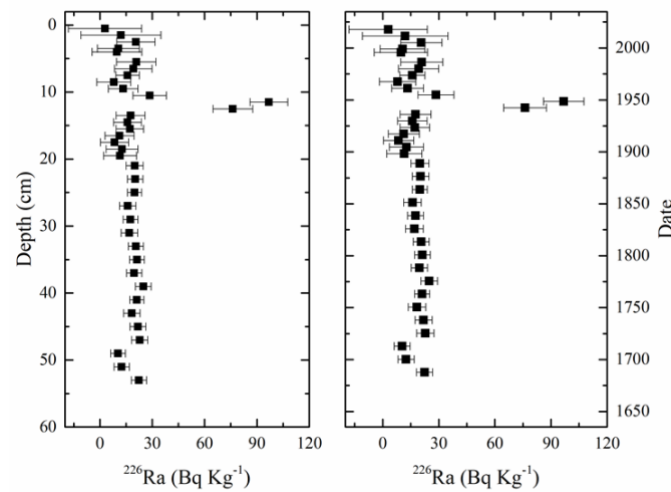


Figure 4. The activity concentration distribution of ^{226}Ra as a function of core depth and date

CONCLUSIONS

This study aimed to use natural and anthropogenic radionuclides to understand the phenomenon of sediment deposition in deep basins and to apply radio-dating methods to a sediment core. According to the measured data, the studied radionuclides proved to be a sufficient tracer for the deep basin of the North Aegean validating that the gravity flows transport and deposit sediment. They are useful for dating the sediment column, the calculation of the accumulation rate, and the identification of possible geophysical phenomena. The activity concentrations of ^{226}Ra and ^{232}Th series show an almost constant distribution, except the 10-12 cm part of the core, which in chronology is estimated between 1950-1960, where the concentration is much higher. The sediment in this section is richer in natural radioactivity, which may be attributed to geophysical incidences after 1950 (seismic activity 1960-70). However, the activity concentration of ^{40}K , in this part of the core, does not change significantly, which suggests that such an event affected only the activity concentrations of the Ra isotopes. The atmospheric deposition of ^{210}Pb in a deep-sea environment was found to be very low. However, the gravity flow of sediment from the slopes of the basin provides additional sediment material. The radio dating method of ^{210}Pb (CF: CS model) proved to be an efficient tool for the estimation of the accumulation rate,

although it was not constant throughout the decades where geophysical events took place. The ^{137}Cs radio dating method was also applied effectively since it validated the results of the ^{210}Pb model.

Acknowledgments

I would like to thank Dr. Kostas Kalfas for providing the SPECTRW analysis program.

References

- [1] G. Eleftheriou, PhD Thesis (2014), National Technical University of Athens, Greece
- [2] A. Arias-Ortiz, et al., Biogeosciences 15, 6791 (2018); doi: 10.5194/bg-15-6791-2018
- [3] P. Dasgupta, Earth-Science Rev. 62, 265 (2003); doi: 10.1016/S0012-8252(02)00160-5
- [4] I.D.L. Foster et al., J. Paleolimnology 35, 881 (2006); doi: 10.1007/s10933-005-6187-6
- [5] G.R. Gilmore, J. Wiley, Practical Gamma-ray Spectrometry 2nd Edition (2011)
- [6] G.F. Knoll and H.W. Kraner, Proceedings of the IEEE (1981); doi:10.1109/PROC.1981.12016
- [7] L. Kölbel et al., Geotherm. Energy 8, 24 (2020); doi: 10.1186/s40517-020-00179-4
- [8] J. Lilley, Nuclear Physics: Principles and Applications, Manchester Physics Series, Wiley (2001)
- [9] M. Lyle, Deep-Sea Sediments BT - Encyclopedia of Marine Geosciences, Springer Netherlands, Dordrecht 1 (2014); doi: 10.1007/978-94-007-6644-0_53-2
- [10] D. Papanikolaou et al., Mar. Geol. 407, 94 (2019); doi: 10.1016/j.margeo.2018.10.001
- [11] G. Postma, Sediment Gravity Flow BT - Encyclopedia of Snow, Ice and Glaciers, 1005 (2011); doi: 10.1007/978-90-481-2642-2_476
- [12] J.A. Sanchez-Cabeza and A.C. Ruiz-Fernández, Geochim. Cosmochim. Acta 82, 183–200 (2012); doi: 10.1016/j.gca.2010.12.024
- [13] Tsoulfanidis, Landsberger, Sheldon, 2015. Measurement and detection of radiation.
- [14] T. Vidmar, NIM A. 550, 603 (2005); doi: 10.1016/j.nima.2005.05.055
- [15] T. Vidmar et al., Appl. Rad. Isot. 69, 908 (2011); doi: 10.1016/j.apradiso.2011.02.042